

Limit State Response of Composite Columns and Beam-Columns

Part 1: Formulation of Design Provisions for the 2005 AISC Specification

ROBERTO T. LEON, DONG KEON KIM, AND JEROME F. HAJJAR

Composite construction exploits the synergistic action in a single structural member of steel in tension and shear and concrete in compression. Additional construction advantages for composite construction accrue from the fact that concrete has relatively low material costs, good fire resistance, and is easy to place, while the steel offers high ductility, toughness and high strength-to-weight and stiffness-to-weight ratios. These advantages have been used extensively in the development of composite floor systems for steel buildings in North America since the late 1950s (Chien and Ritchie, 1984, 1993; Smith and Coull, 1991; Viest, Colaco, Furlong, Griffis, Leon, and Wyllie, 1997; Taranath, 1998). In composite floors, the concrete carries the compressive forces, the steel carries the tensile ones, and direct bond, steel shear connectors, or other mechanisms are used to transfer the horizontal shears between the two. As compared to composite floor systems, composite columns, composite walls, and other full vertical and horizontal composite structural systems are not as popular in the United States, although they are extensively used in Japan and the Far East (Uy, 1998; Morino, Uchikoshi and Yamaguchi, 2001). In Japan and China they are used in buildings of all heights primarily because of their seismic resistance; in the rest of Asia they are often used in tall buildings to reduce drift due to typhoon (hurricane) winds.

There are two basic kinds of composite columns: steel sections encased in concrete (also termed encased composite sections, steel-reinforced concrete sections, or SRC) and steel sections filled with concrete (also termed filled

composite sections, concrete-filled tubes, or CFT). The latter can be either circular (CCFT) or square or rectangular (RCFT) in cross section. In composite columns, additional synergies to those listed above are possible because: (a) in CFT construction, the steel increases the strength and ductility of the concrete because of its confining effect, the concrete inhibits local buckling, and the concrete formwork can be omitted; and (b) in SRC construction, the concrete delays failure by local buckling and acts as fireproofing. Typically, the use of composite columns in the United States (U.S.) has been limited to mega-columns or perimeter frames in tall buildings in seismic or hurricane areas where lateral drift controls design (Viest et al., 1997; Roeder, 1998; Galambos, 2000). In these cases, the steel column is often used to carry the gravity loads during construction, and is later encased or filled with concrete to provide lateral stiffness (Figure 1). A typical cross section for a mega-column, in this case from the 19th floor of the Norwest Center in Minneapolis, Minnesota, is shown in Figure 2 (Leon and Bawa, 1990, 2002).

Composite columns represent a very attractive option for the increase of building strength, stiffness and deformation capacity in structures subjected to large man-made and natural lateral loads. Four reasons can be identified for the lack of use of composite columns in the United States. First, they straddle both steel and concrete design but currently there are no simple, unified design provisions that will allow either the use of a composite column with a large steel reinforcement ratio (for example, greater than 8%) in reinforced concrete construction or one with a low steel reinforcement ratio (for example, less than 4%) in a steel building. Second, there has not been a concerted effort to update design provisions for many years despite the fact that a substantial amount of both experimental and analytical research have been carried out worldwide. Third, there is a lack of design aids and examples to help engineers unfamiliar with composite columns to explore their use as an alternative to conventional steel or reinforced concrete columns. Fourth, because of variations in construction industry practices related to separation of trades across the U.S., the economies of composite construction cannot always be realized. The 2005 AISC *Specification for Structural Steel Buildings*, ANSI/AISC 360-05 (AISC, 2005b), hereafter referred to as the AISC *Specification*,

Roberto Leon is professor, school of civil and environmental engineering, Georgia Tech, Atlanta, GA, and former chair, AISC task committee 5 on composite construction.

Dong Keon Kim is Ph.D. candidate, department of civil, structural and environmental engineering, The University at Buffalo, Buffalo, NY.

Jerome F. Hajjar is professor, department of civil and environmental engineering, University of Illinois, Urbana, IL.

addresses directly the first two issues, and this paper provides a detailed background to their development. A companion paper by Leon and Hajjar (2007), and forthcoming in the *Engineering Journal*, provides design examples and discussions to complement the examples included in the new AISC *Steel Construction Manual* (AISC, 2005c).

OBJECTIVES

The 2005 AISC *Specification* (AISC, 2005b) present a completely new approach for the design of composite columns within the context of U.S. load and resistance factor design (LRFD) provisions, in addition to extending its use to the allowable strength design (ASD) methodology. The overall goals of the new provisions were two-fold. The first goal was to develop a seamless design procedure for structural composite members subjected to combined flexure, axial force, shear and torsion ranging from a typical reinforced concrete beam-column (ACI, 2005) to a typical steel beam-column (AISC, 2005b). The new provisions permit for the design of a composite column with a total reinforcement ratio ranging from 1% to a practical upper limit in the vicinity of 16%. This goal was achieved in a straightforward fashion at the cross-section strength level, but the differences in the stability approaches taken by ACI (ACI, 2005) and AISC (AISC, 2005b) still need to be reconciled. The second goal was to improve and modernize the AISC composite column provisions. The previous design provisions for composite columns (AISC, 1999) were based on procedures developed

in the 1970s (Ravindra, and Galambos, 1978; Hansell, Galambos, Ravindra, and Viest, 1978; SSRC, 1979; Viest et al., 1997). In this prior work, an approach was used in which the composite beam-column was converted to an equivalent steel beam-column. This approach was logical as the provisions originally intended to address columns with relatively high steel reinforcement ratios (for example, greater than 4%) and therefore it was a natural approach to tie their stability design to the established column curves for steel members. This approach has been shown to yield comparatively low reliability indices (Lundberg and Galambos, 1996; Leon and Aho, 2002), with particularly large dispersions for some types of beam-columns. In addition, these provisions were cast in LRFD format and never formally transferred to an ASD format. This is despite the fact that the original formulas proposed in SSRC (1979) were in ASD format. The new provisions address these discrepancies by first developing a comprehensive database of composite column experiments and then utilizing this database to calibrate new design provisions.

DATABASE OF BEHAVIOR OF COMPOSITE COLUMNS AND BEAM-COLUMNS

The development of the database (Kim, 2005) for the 2005 AISC *Specification* started with a general update of the database developed by Aho (Aho, 1997; Leon and Aho, 2002). Initially, the database was populated with as many tests as possible found in the open literature; for example, no effort was made to limit the database to tests that complied with the material and geometric limitations present in current specifications. In addition, both tests subjected to monotonic

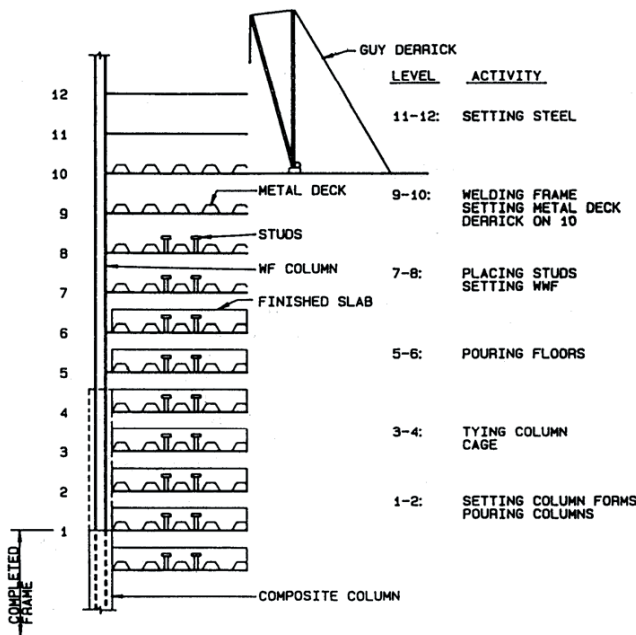


Fig. 1. Construction process for composite frame (Viest et al., 1997).

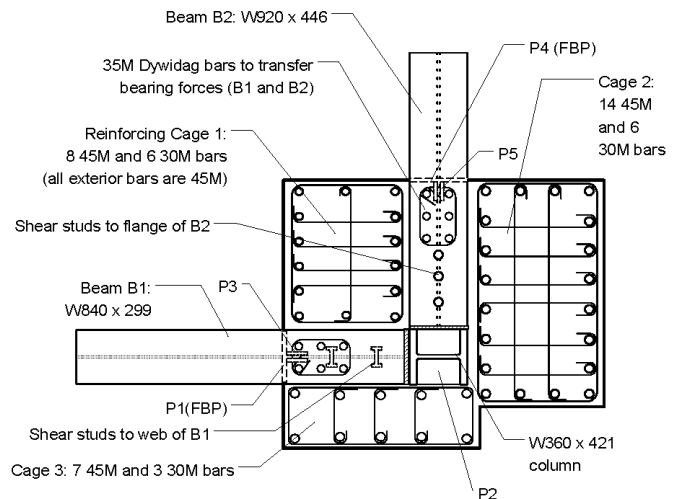


Fig. 2. Composite column used in the Norwest Center (Minneapolis, Minnesota) (Leon and Bawa, 2002).

Table 1. Composite Column and Beam-Column Database Summary

	SRC		Circular CFT		Rect. CFT	
	Cols.	Beam-Cols.	Cols.	Beam-Cols.	Cols.	Beam-Cols.
Total No. of Tests	119	136	312	198	222	194
No. of Tests for Analysis	89	117	210	118	103	62
Maximum F_y (ksi)	72.7	58.0	121.0	70.0	120.8	108.8
Minimum F_y (ksi)	32.4	32.3	32.1	27.5	36.9	36.8
Maximum f'_c (ksi)	9.5	6.8	16.5	16.3	14.9	14.9
Minimum f'_c (ksi)	1.8	1.8	2.6	2.9	2.6	4.2
Maximum L/r	466.7	247.2	133.8	87.1	91.1	91.2
Maximum ρ_{ss}	12.9%	14.6%	27%	46.6%	26.6%	24.9%
Minimum ρ_{ss}	2.7%	14.6%	5.5%	5.1%	7.1%	11.1%

or cyclic loading, with both single and double curvature, and with both proportional and nonproportional loading were included (proportional loading refers to loading in beam-columns whereby an eccentric axial load is applied—thus the axial load and bending moment increase in a fixed ratio to each other).

The first step in selecting the tests to be used for the development of new design equations was to eliminate from the database specimens that for one reason or another were deemed to be outside the scope of the work. Only tests that clearly fell outside the parameters were eliminated, and every effort was made at retaining as many tests as possible. This is a different approach from calibration efforts such as those carried out for Eurocode (Eurocode, 2004), where only a small subset of very well-detailed tests was used (Roik and Bergmann, 1988). Both approaches are valid, but the choice made here was based on the assumption that many of the problems encountered in testing (for example, accidental load eccentricities and the effects of friction at the ends) may reflect actual imperfections in practice. Because much of the effort in this work was geared towards comparing different specifications, the effect of any outlier data is assumed to be small in the comparisons (in other words, all approaches are assumed to be impacted equally by outlier data).

The most important categories of experiments that were established at this stage were:

- Specimens that did not achieve their ultimate strength due to well-documented problems during testing. These were the only tests that were completely eliminated from further analysis.
- Tests in which the specimens were subjected to cyclic loading, as these are often designed to be shear critical and subjected to double curvature. These specimens will be examined in a future work as part of an assessment of the provisions of the AISC *Seismic Provisions for Structural Steel Buildings* (AISC, 2005a).

Specimens in the following categories were also removed and analyzed separately:

- Tests subjected to biaxial bending.
- Tests subjected to unequal end moments.
- Tests that did not meet applicable local buckling criteria.
- Tests containing lightweight concrete.

Table 1 summarizes a number of the key parameters of the database. While the table shows a wide range of parameters, the available data is often clustered. As an example, Figure 3 shows a scatter diagram indicating the available data for encased composite beam-columns as a function of concrete strength, steel yield strength, and overall reinforcement ratio. The diagram shows considerable clustering around steel strengths of 36 ksi, concrete strengths of 2.5 ksi to 5 ksi, and reinforcement ratios of 5%, 8%, and 13%. Other portions of the figure show few if any tests.

DEVELOPMENT OF DESIGN EQUATIONS FOR COMPOSITE COLUMNS

In the first phase of the work, a statistical approach was taken in an effort to match the test data as well as possible. In this effort, several assumptions were necessarily made about generating cross-section strength values and coefficients to account for length effects (Leon and Aho, 2002; Kim, 2005). To assess cross-section strength, the plastic strength approach proposed by Eurocode 4 (Roik and Bergmann, 1992; Eurocode, 2004) was adopted, because (1) it is conceptually in agreement with the ultimate strength assumptions permitted under both the ACI 318 (ACI, 2005) and ANSI/AISC 360-05 (AISC, 2005b) provisions, and (2) it has shown excellent correlation to tests of short columns in the past.

For the length effects, the main efforts were aimed at (1) generating an accurate expression for the equivalent rigidity

(EI_{equiv}) of the column for the calculation of axial compressive strength for either elastic or inelastic flexural buckling, and (2) developing a new column curve based on those results. Item (2) reflects the fact that it has long been recognized that the typical steel column stability curve does not match composite beam-columns well. For example, Eurocode 4 (Eurocode, 2004) has three separate column curves for composite members: one is for encased steel columns bent about the strong axis, one is for encased steel columns bent about the weak axis, and one is for concrete-filled steel sections. From this effort, the following recommendations were developed.

The design compressive strength, $\phi_c P_n$, and allowable compressive strength, P_n/Ω_c , for axially-loaded encased composite columns shall be determined based on the column slenderness, α , as follows:

$$\alpha = \sqrt{(P_o / P_e)} \quad (1)$$

For SRC,

$$P_o = A_s F_y + A_{sr} F_{yr} + 0.85 A_c f'_c, \text{ kips (kN)} \quad (\text{AISC 2005 I2-4})$$

For RCFT and CCFT,

$$P_o = A_s F_y + A_{sr} F_{yr} + C_2 A_c f'_c, \text{ kips (kN)} \quad (\text{AISC 2005 I2-13})$$

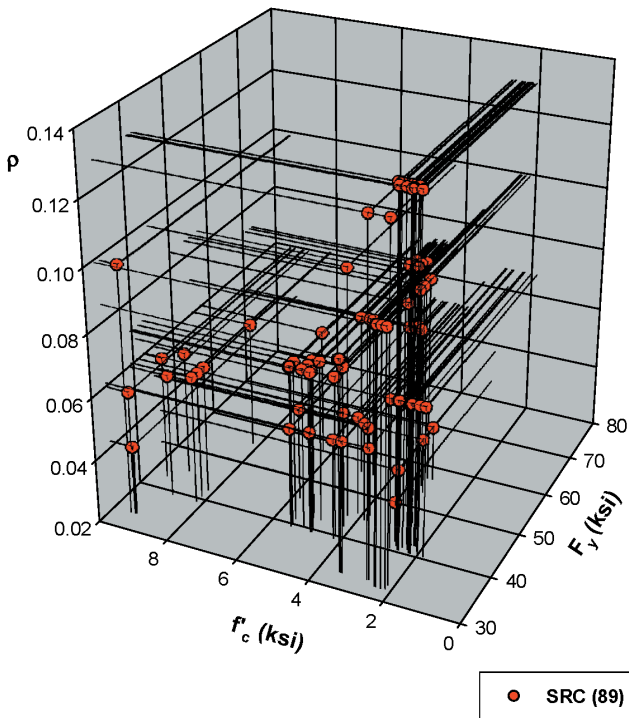


Fig. 3. Scatter diagram showing available data for SRC columns as a combination of concrete and steel strengths (ksi) and reinforcement ratio.

$$P_e = \pi^2(EI_{eff}) / (KL)^2, \text{ kips (N)} \quad (\text{AISC 2005 I2-5})$$

$$EI_{eff} = E_s I_s + E_s I_{sr} + 0.2 E_c I_c, \text{ kip-in.}^2 \text{ (N-mm}^2\text{)} \quad (2)$$

where

- A_s = area of the steel section, in.² (mm²)
- A_c = area of concrete, in.² (mm²)
- A_{sr} = area of continuous reinforcing bars, in.² (mm²)
- E_c = modulus of elasticity of concrete = $w_c^{1.5} \sqrt{f'_c}$, ksi (0.43 $w_c^{1.5} \sqrt{f'_c}$, MPa)
- E_s = modulus of elasticity of steel = 29,000 ksi (210 MPa)
- EI_{eff} = effective moment of inertia of composite section, kip-in.² (N-mm²)
- f'_c = specified minimum compressive strength of concrete, ksi (MPa)
- F_y = specified minimum yield stress of steel section, ksi (MPa)
- F_{yr} = specified minimum yield stress of reinforcing bars, ksi (MPa)
- I_c = moment of inertia of the concrete section, in.⁴ (mm⁴)
- I_s = moment of inertia of steel shape, in.⁴ (mm⁴)
- I_{sr} = moment of inertia of reinforcing bars, in.⁴ (mm⁴)
- K = the effective length factor determined in accordance with Chapter C
- L = laterally unbraced length of the member, in. (mm)
- w_c = weight of concrete per unit volume ($90 \leq w_c \leq 150$ lbs / ft³ or $1500 \leq w_c \leq 2500$ kg/m³)
- C_2 = 0.85 for rectangular sections and 0.95 for circular sections
- P_o = nominal compressive axial strength without consideration of length effects, kips (N)

When $\alpha \leq 0.5$

$$P_n = P_o, \text{ kips (N)} \quad (3)$$

When $0.5 < \alpha \leq 1.5$

$$P_n = P_o (\alpha^{-0.4} - 0.32), \text{ kips (N)} \quad (4)$$

$$\phi_c = 0.75 \text{ (LRFD)} \quad \Omega_c = 2.00 \text{ (ASD)}$$

where

- P_n = nominal axial strength, kips (N)
- ϕ_c = resistance factor for compression
- Ω_c = safety factor for compression

Encased composite columns that have $\alpha > 1.5$ are permitted when their use is justified by analysis or testing.

The calibration results of these early efforts were encouraging, but it should be noted that the new Equations 3 and

4 are purely empirical in nature. These equations, while giving good results, did not provide any continuity with existing steel design provisions (in other words, as the amount of concrete decreased, these equations did not tend towards the nominal axial compressive strength for steel columns). Equations 3 and 4 thus reflected the different shape of the stability curve for composite sections. Moreover, due to a dearth of very slender members in the experimental database, the equations had to be limited to a value of the slenderness parameter α of 1.5. These limitations meant that the proposed provisions lacked sufficient generality to be included in the 2005 AISC provisions.

It was determined that the best approach would be to default to the existing AISC column curve, and thus a second round of calibration was undertaken. In this case, the single objective was to refine the definition of the EI_{eff} to provide as good a match as possible while utilizing the AISC column curve. The work resulted in expressions for EI_{eff} that were complex. For example, the resulting equation for the equivalent rigidity of encased composite sections was

$$EI_{eff} = \left(0.313 + 0.00334 \frac{L}{h} - 0.203 \frac{e}{h} \right) \times E_c (I_g - I_s - I_{sr}) + 0.729 E_s I_s + 0.788 E_s I_{sr} \quad (5)$$

where

- L = length of the member
- h = cross section dimension perpendicular in the plane of buckling
- e = eccentricity of the axial force (in other words, the ratio of the flexural moment to the axial compressive force)
- E_c and E_s = moduli of elasticity of the steel and concrete, respectively
- I_g , I_s , and I_{sr} = gross moment of inertia of the entire section, of the steel section, and of the steel reinforcing bars, respectively

This equation shows the main parameters that influence the buckling behavior of these members. The equation is also similar in format, albeit with different coefficients, to ones proposed by Mirza and Tikka (1999) for SRC sections. The Mirza and Tikka expression may be reduced without significant loss of accuracy to

$$EI_{equiv} = \left(0.3 - 0.2 \frac{e}{h} \right) E_c (I_g - I_s - I_{sr}) + 0.8 (E_s I_s + E_s I_{sr}) \quad (6)$$

This form of the equation, however, is not useful for design as it requires a separate calculation for each load combination based on the resulting eccentricity (in other words, moment-to-axial compression ratio) in the cross section. It was

thus decided to accept a simpler equation for what is termed in the specification as an effective stiffness of the composite section, EI_{eff} . For SRC and CFT sections, respectively, the resulting equation was

$$EI_{eff} = E_s I_s + 0.5 E_s I_{sr} + C_1 E_c I_c \quad (\text{AISC 2005 I2-6})$$

$$EI_{eff} = E_s I_s + 1.0 E_s I_{sr} + C_3 E_c I_c \quad (\text{from AISC 2005 I2-14})$$

In Equation (AISC 2005 I2-6), the contribution of the reinforcing steel is halved because it is assumed from symmetry that at least that portion of the bars in SRC sections will be yielding and not contributing to the rigidity. The added confinement for CFTs raises that factor to 1.0 in Equation (AISC 2005 I2-14). The factors on the concrete section, C_1 , and C_3 , are meant to reflect the cracked nature of the section when a stability limit is reached. The data indicates that in a statistical sense this effect is roughly proportional to the area of the steel section. Thus, for encased composite columns (SRC)

$$C_1 = 0.1 + 2 \left(\frac{A_s}{A_c + A_s} \right) \leq 0.3 \quad (\text{AISC 2005 I2-7})$$

and for filled composite columns (CFT)

$$C_3 = 0.6 + 2 \left(\frac{A_s}{A_c + A_s} \right) \leq 0.9 \quad (\text{AISC 2005 I2-15})$$

However, the relationship between the effectiveness of the concrete and the ratio of the areas is probably more a reflection of the types of columns present in the database than an actual mechanistic behavior. The limit of $r < 0.3h$ (in other words, the radius of gyration should be less than 30% of the dimension in the plane of buckling) that was present in previous versions of the AISC *Specification* (AISC, 1999) was dropped as no reasonable mechanistic justification for that limit could be found.

While the formats are different, there are no large inconsistencies between Equations 6 and Equations (AISC 2005 I2-6) and (AISC 2005 I2-14). The upper limit for the contribution of the concrete is $0.3E_c I_c$ from Equation 6 if the eccentricity is small, and the same is true from Equation (AISC 2005 I2-7) if the reinforcement ratio is large. The lower contribution from the reinforcing bars in Equation (AISC 2005 I2-6) as compared to Equation 6 is compensated by using the full value of the contribution from the steel section as opposed to 80% of the value as given in Equation 6. Because the reinforcing bars tend to be located farther away from the plastic neutral axis than the steel section, they contribute substantially more to the strength and stiffness than their area would indicate (in other words, their value of $A_{sr} d_i$ and $A_{sr} d_i^2$ is large). In Equations (AISC 2005 I2-7) and (AISC 2005 I2-15), the contribution of any reinforcing bars to the

steel area is ignored because there was insufficient data to assess its effects (in other words, there were few tests with large amounts of reinforcing bars or with continuous bars lumped at the corners to help establish an upper limit to their contribution). This issue will be revisited in the future and it is likely that the term A_s could be changed to $A_{s,total}$.

The use of Equations (AISC 2005 I2-6), (AISC 2005 I2-7), (AISC 2005 I2-14), and (AISC 2005 I2-15), which allow the engineer to approximate the component contributions, as opposed to a more complex equation (for example, Equations 5 or 6) leads to the first reduction in accuracy in the design equation. The second loss in accuracy is introduced when adopting the reduction equation to account for stability effects. The EI_{eff} computed from Equations (AISC 2005 I2-6) and (AISC 2005 I2-14) in the 2005 AISC *Specification* (AISC, 2005b), is used here to calculate a slenderness parameter, λ , which is then used to compute the reduction due to slenderness effects as follows:

$$\lambda = \sqrt{\frac{P_o}{P_e}} \quad \text{or} \quad \lambda^2 = \frac{P_o}{P_e} \quad (7)$$

$$P_o = A_s F_y + A_{sr} F_{yr} + 0.85 A_c f'_c \quad (\text{or } 0.95 A_c f'_c \text{ for CCFTs})$$

$$(AISC 2005 I2-4; AISC 2005 I2-13)$$

$$P_e = \pi^2 (EI_{eff}) / (KL)^2 \quad (AISC 2005 I2-5)$$

For $\lambda \leq 1.5$

$$P_n = 0.658 \lambda^2 P_o = 0.658 \left(\frac{P_o}{P_e} \right) P_o \quad (8)$$

For $\lambda > 1.5$

$$P_n = \left(\frac{0.877}{\lambda^2} \right) P_o = 0.877 P_e \quad (9)$$

$$\phi_c = 0.75 \text{ (LRFD)} \quad \Omega_c = 2.00 \text{ (ASD)} \quad (10a)$$

The resistance and safety factors for flexure will also be used in the following sections in the discussion of beam-columns. Within ANSI/AISC 360-05 (AISC, 2005b) for composite beam-columns these values are:

$$\phi_b = 0.90 \text{ (LRFD)} \quad \Omega_b = 1.67 \text{ (ASD)} \quad (10b)$$

Equations 8 and 9 are equivalent to Equations I2-2 and I2-3 for composite columns and Equations E3-2 and E3-3 for steel columns in the 2005 AISC *Specification* (AISC, 2005b), albeit using a different format. The decision to maintain the form of the AISC column curve for steel columns [Equations E3-2 and E3-3 of ANSI/AISC 360-05 (AISC, 2005b)] in Equations 8 and 9 leads to a further loss of accuracy in comparison with the tests.

DESIGN COMPARISONS AND CALIBRATION FOR COMPOSITE COLUMNS AND BEAM-COLUMNS

For calibration and comparison of composite beam-column strength, three procedures were used: the existing 1999 AISC *LRFD Specification for Structural Steel Buildings* (AISC, 1999), the 2005 AISC *Specification* (AISC, 2005b) and Eurocode 4 (Eurocode, 2004). To calculate the axial force-thrust (moment) interaction diagram, several procedures can be used, as described in more detail in the companion article (Leon and Hajjar, 2007, and forthcoming in the *Engineering Journal*).

The first is a cross-sectional analysis that utilizes a strain compatibility approach and nonlinear material properties. This is shown as a heavy black line in Figure 4 for the case of a maximum concrete strain of 0.003. A rigid-plastic approach with some simplifying assumptions leads to the approximate interaction diagram shown as a dotted line in Figure 4. This latter approach was chosen as the basis for further work.

The simplified interaction curve (Figure 4) was calculated by first assuming the plastic strength was achieved throughout the cross section, and then the resulting curve was approximated by a multilinear curve as shown in the figure. Point A represents the plastic axial compressive strength of the column. Point B is characterized by the condition in which there is no net axial force. At Point C, the moment resistance is of the same magnitude as at point B, but the resistance to axial force is taken as that of the concrete portion only. Point D corresponds to an estimate of the maximum moment because the neutral axial lies in the center of the cross section (for doubly symmetric sections).

For the comparisons for beam-columns, the first step was to compute P_o based on Equations (AISC 2005 I2-4) and (AISC 2005 I2-13). The slenderness reduction, λ , (Equation 7) was then applied and the compressive axial strength for the column was reduced from point i to point i_λ (where $i = A, B, C, D, E$). Finally, the resistance factor, ϕ_c , was applied, and the compressive axial strength was thus reduced from i_λ to i_d . The flexural strength of the section was also reduced by a resistance factor, ϕ_b , from point i to point $\phi_b i$. This procedure produced a design envelope, shown as a dashed-dotted line in Figure 4. A representative test result is also shown as point F_λ in the figure. Typically, these values lie outside the ultimate predicted strength interaction diagram due to over-strength as compared to perfectly-plastic calculations.

As most of the tests in the database did not report a true moment or the deflections along the specimen at failure, the second-order effects could not be directly included in the calibrations. This fact led to the selection of the reported maximum axial load and the initial loading eccentricity (F_λ and e in Figure 5) as the calibration parameters in these studies. In Figure 5, the dotted line (O to F_λ) represents the actual test load path, including second-order effects. The heavy solid line represents the ultimate strength envelope at large

strains ($\epsilon_c \gg 0.003$ and $f_s > F_y$, where ϵ_c is the compressive strain at the extreme compression fiber in the concrete and f_s is the tensile strain at the extreme tension fiber in the steel section) including length and confinement effects. The point chosen as the calibration point (H_λ) corresponds to the intersection of the failure load (P_{exp}) with the line of constant eccentricity (e). The values of axial load and moment for this point are less than those at failure for constant eccentricity with no second-order effects (Point I_λ), and the moment is

less than that considering second-order effects (Point F_λ). Thus this choice can be considered to be conservative for tests above the balanced failure point, which constituted the overwhelming majority of the tests in the database. In addition, because of testing constraints, most tests have been run with relatively large axial loads and small eccentricities. Thus the differences between Points F, H, and I are probably much smaller than those shown schematically in Figure 5. The comparisons were made both with and without

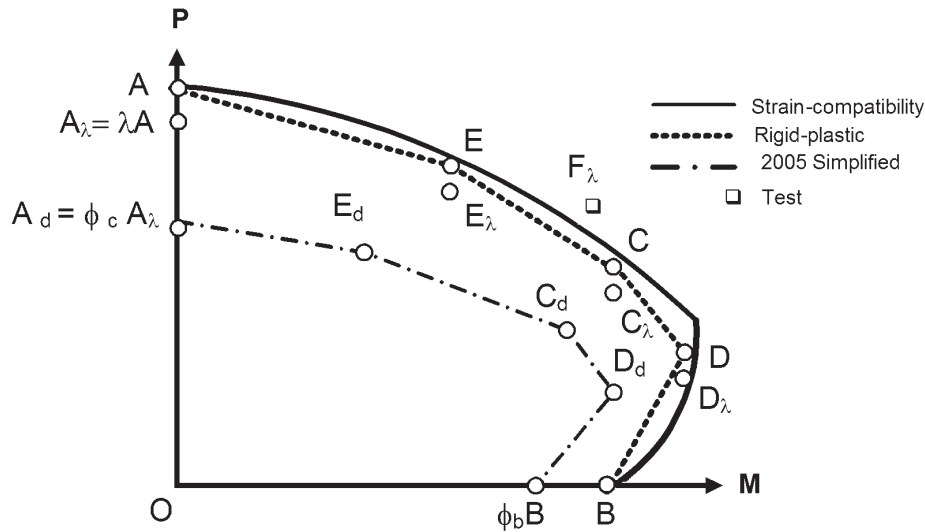


Fig. 4. Interaction diagrams for composite beam-columns.

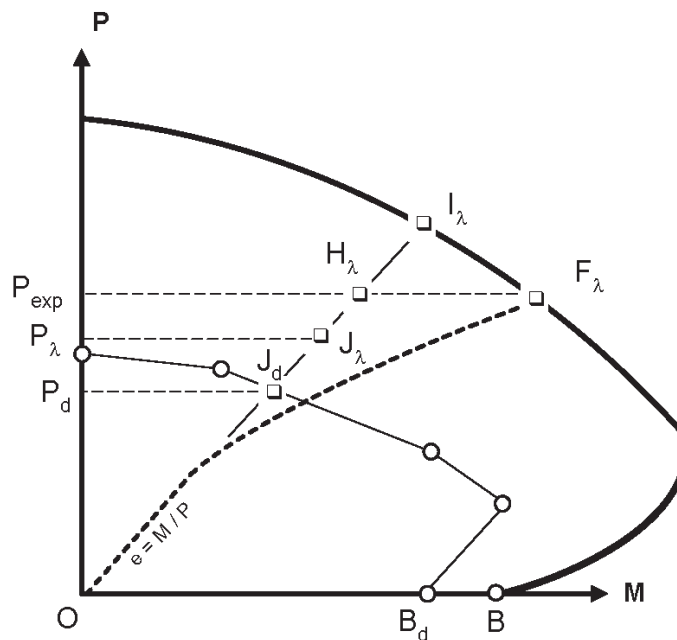


Fig. 5. Definition of ultimate strength values from experimental tests.

Table 2. Comparison of Test-to-Predicted Ratios for Axial Compressive Strength from the Composite Beam-Column Database

Type		No. of Tests	Mean	Standard Deviation	COV	Mean Design Axial Load AISC 2005 Mean Design Axial Load AISC 1999 (COV)
Encased columns (SRC)	AISC 1999	89	1.22	0.19	0.16	1.11 (0.15)
	AISC 2005		1.18	0.20	0.17	
	Eurocode 4 (2004)		1.09	0.14	0.13	-
Encased beam-columns (SRC)	AISC 1999	117	1.41	0.32	0.23	0.82 (0.23)
	AISC 2005		1.03	0.25	0.24	
	Eurocode 4 (2004)		1.21	0.22	0.18	-
Circular CFT columns (CCFT)	AISC 1999	210	1.28	0.19	0.15	1.08 (0.04)
	AISC 2005		1.23	0.18	0.15	
	Eurocode 4 (2004)		1.06	0.18	0.17	-
Circular CFT beam-columns (CCFT)	AISC 1999	118	1.49	0.33	0.22	0.88 (0.21)
	AISC 2005		1.14	0.22	0.19	
	Eurocode 4 (2004)		1.25	0.19	0.15	-
Rectangular CFT columns (RCFT)	AISC 1999	103	1.06	0.12	0.11	1.13 (0.01)
	AISC 2005		1.06	0.12	0.11	
	Eurocode 4 (2004)		0.99	0.12	0.12	-
Rectangular CFT beam-columns (RCFT)	AISC 1999	62	1.27	0.33	0.26	0.87 (0.12)
	AISC 2005		0.99	0.28	0.28	
	Eurocode 4 (2004)		1.19	0.40	0.34	-

resistance factors (labeled as unfactored and factored cases, respectively), as these vary considerably from code to code. The ratios used in the comparisons then become P_{exp}/P_{λ} and P_{exp}/P_d for the unfactored and factored cases, respectively. The predicted values (P_{λ} and P_d) were calculated by interpolation between the simplified points of interaction diagram.

Two final points need to be made about these studies. First, attempts to optimize the AISC (2005b) design provisions to both the column and beam-column data simultaneously proved challenging. The provisions were thus developed to match as best as possible the column case and then checked for the beam-column case. Second, for circular and rectangular concrete-filled sections, local buckling checks were also carried out. These checks were used to verify that the new limits on local buckling proposed in the 2005 AISC Specification (AISC, 2005b) were reasonable. These checks are discussed in the next section.

Table 2 shows comparisons of the predicted results by the three specifications for the specimens in the reduced database (see Number of Tests for Analysis in Table 1). Figures 6 thru 8 give the results for encased beam-columns for AISC (1999), AISC (2005b), and Eurocode 4 (Eurocode, 2004), respectively. In each figure, the abscissa corresponds to the slenderness parameter by each of the respective codes [in other words, λ_c from Equation E2-4 in AISC (1999); λ in Equation 7 above, corresponding to the formulas for P_n , Equations I2-2 and I2-3 in AISC (2005b); and $\bar{\lambda}$ in Equation 6.39 in Eurocode 4 (Eurocode, 2004); see these corresponding references for detailed definitions of these slenderness parameters]; the ordinate corresponds to the experimental value of strength, P_{exp} , normalized by the predicted value of strength, P_{pred} , from the corresponding code [in other words, Equations E2-1 with I2-1 and I2-2 in AISC (1999); Equations 8 and 9 above, corresponding to the formulas for P_n ,

Equations I2-2 and I2-3, in AISC (2005b); and Equation 6.30 in Eurocode 4 (Eurocode, 2004)], adjusted to account for the contribution of flexure as described above, without any resistance factors. Table 2 tabulates the corresponding mean and standard deviations and COV value of these ordinate values.

From examining Table 2 and the figures for all cases, similar to Figures 6 through 8, it can be concluded that in general Eurocode 4 (Eurocode, 2004) gives good predictions for columns and the ANSI/AISC 360-05 (AISC, 2005b) method performs well for beam-columns. For rectangular CFT columns, all three methods predict the ultimate strength well. The main improvement for the approach in ANSI/AISC 360-05 (AISC, 2005b) is its ability to handle specimens that have high yield stress, high strength concrete, or both. When comparing design values (in other words, including the resistance factor) the mean value predicted by AISC (1999) is larger than that from ANSI/AISC 360-05 (AISC, 2005b) method for SRC, CCFT and RCFT columns. However, the mean value predicted by AISC (1999) is smaller than that from the ANSI/AISC 360-05 (AISC, 2005b) method for SRC, CCFT and RCFT beam-columns. Figure 9 shows a comparison of the design values for all the specimens in the database, with no resistance factors.

Figure 10 shows a specific design case. Note that care needs to be exercised when interpreting this figure as the values of the slenderness parameters vary. The ratio of the slenderness parameter of ANSI/AISC 360-05 (AISC, 2005b) to that in AISC (1999) and Eurocode 4 (Eurocode, 2004), summarized in conjunction with Figures 6 through 8, is on the

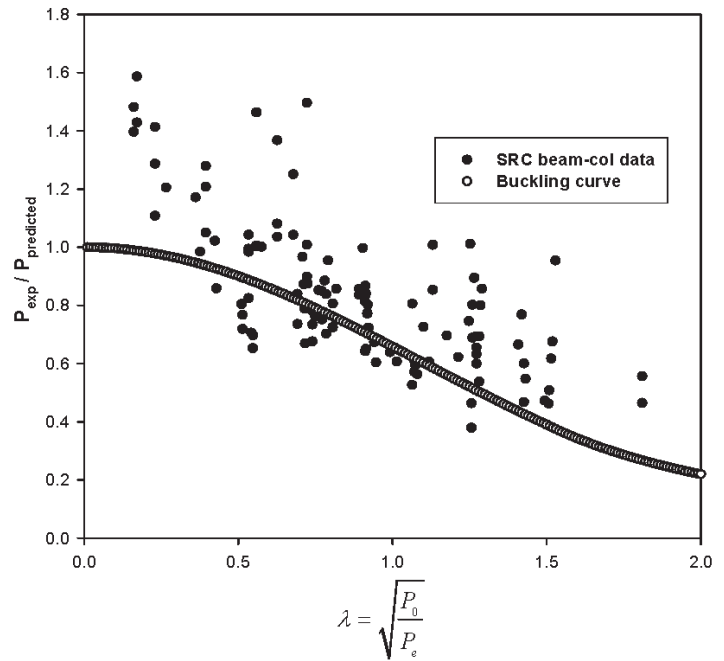


Fig. 7. Ratios of test-to-predicted values for SRC based on ANSI/AISC 360-05 (AISC, 2005b) (Kim, 2005).

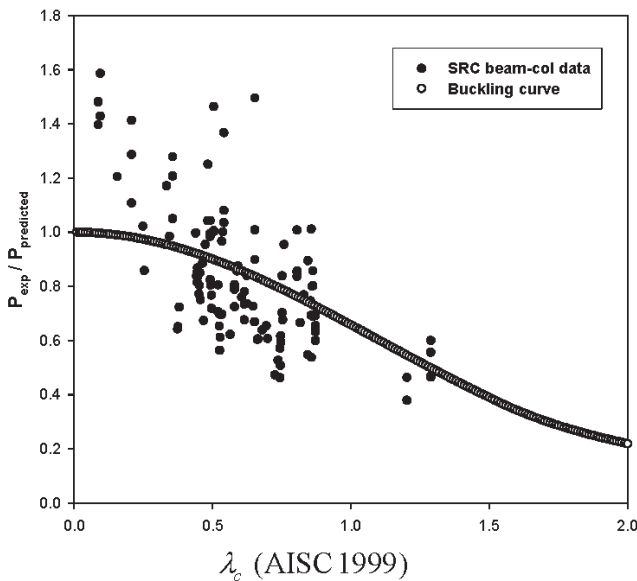


Fig. 6. Ratios of test-to-predicted values for SRC based on AISC (1999) (Kim, 2005).

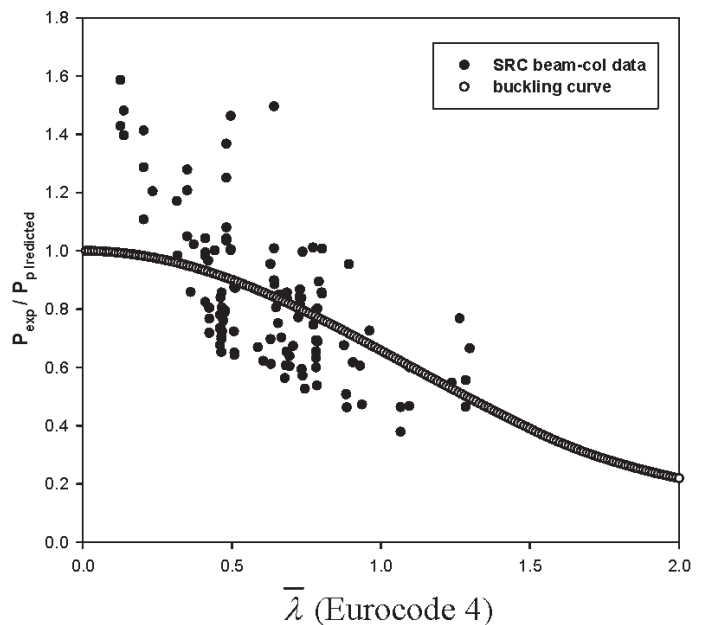


Fig. 8. Ratios of test-to-predicted values for SRC based on Eurocode 4 (Eurocode, 2004) (Kim, 2005)

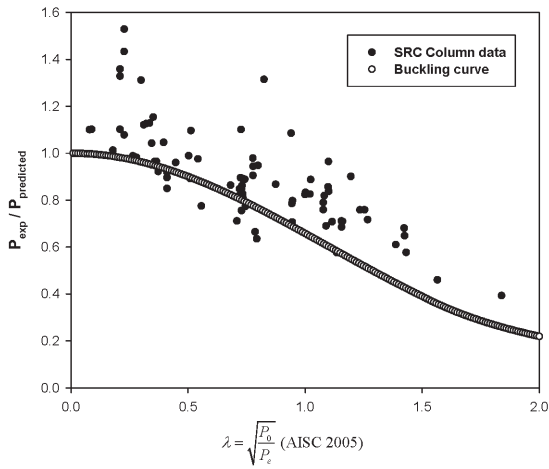


Fig. 9(a). SRC columns.

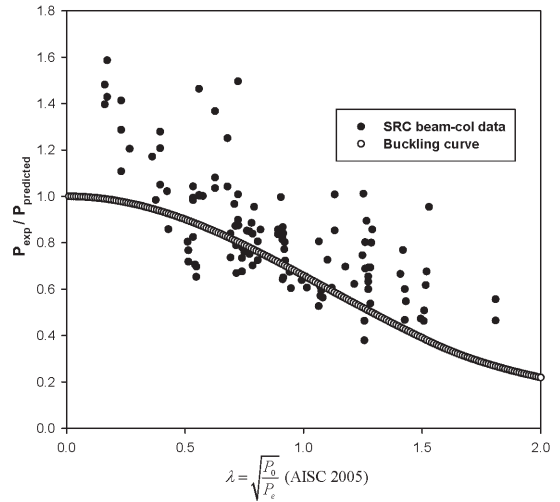


Fig. 9(b). SRC beam-columns

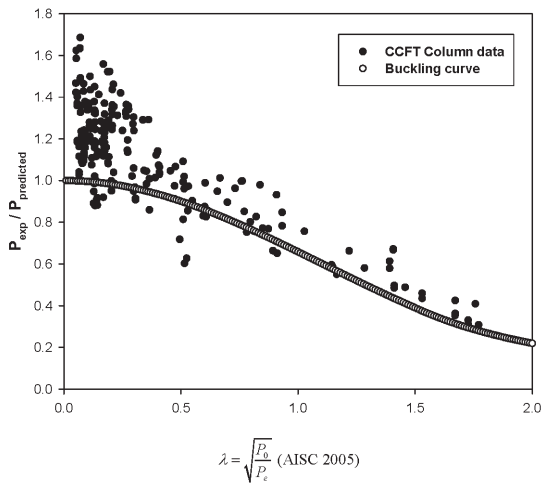


Fig. 9(c). CCFT columns.

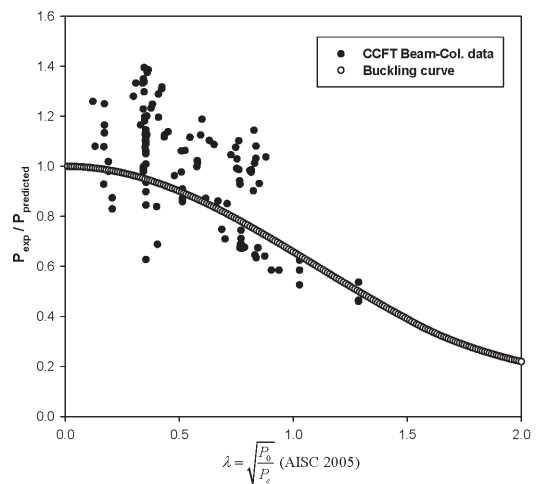


Fig. 9(d). CCFT beam-columns.

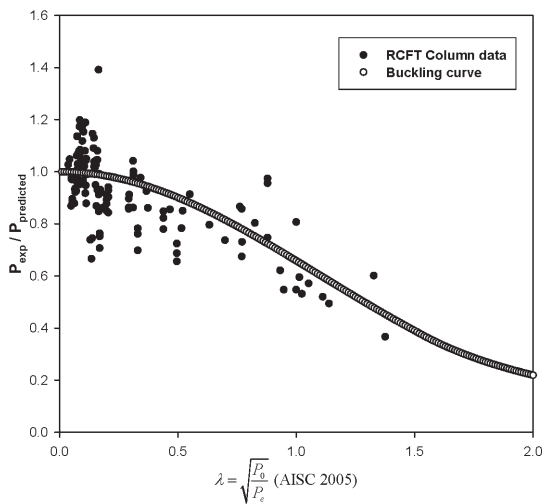


Figure 9(e) RCFT columns
Fig. 9(e). RCFT columns.

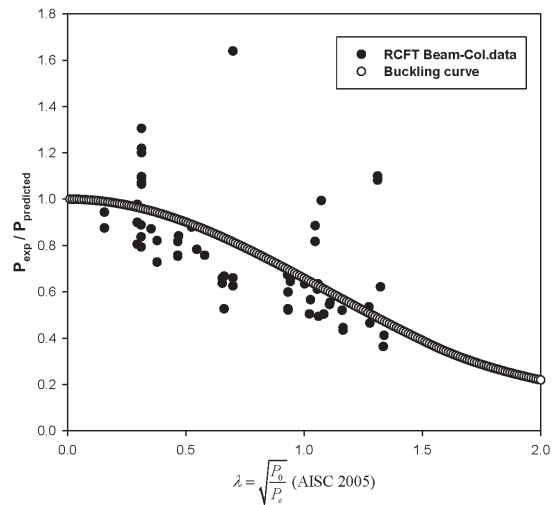


Fig. 9(f). RCFT beam-columns.

Fig. 9 Ratios of test-to-predicted values based on AISC (2005b).

order of 1.4 for SRC sections. Thus the value of the slenderness parameter on the abscissa shown for the “AISC 2005” at a value of 1.4 is roughly comparable to that of both “AISC 1999” and Eurocode 4 at a value of 1.0. For CFTs, the values of the slenderness parameters are similar for all three cases.

LOCAL BUCKLING

An important benefit of the 2005 AISC *Specification* provisions is the liberalization of the local buckling limits for tube wall thickness in CFTs that were published in prior editions of the AISC *Specification* (AISC, 1993; AISC, 1999). Typical allowable slenderness has been increased by approximately 40% for CCFTs and approximately 30% for RCFTs from the previous edition of the AISC *Specification* (AISC, 1999). The evolution of width-to-thickness ratios from the limits given in the 1993 AISC *LRFD Specification for Structural Steel Buildings* (AISC, 1993) to those of the current edition of the AISC *Specification* (AISC, 2005b) for hollow structural sections under uniform compression is shown in Table 3. In addition, the actual limits for the most common hollow structural section (HSS) material (A500 Grade B, $F_y = 42$ ksi for circular HSS and $F_y = 46$ ksi for rectangular HSS) are also included.

The local buckling limits for CFT sections that appeared previously (AISC, 1993) were largely based on SSRC TG20

(SSRC, 1979), which suggested limits for wall slenderness based on available test data. Comparison of the suggested values for composite and noncomposite sections in AISC (1993) suggests an inconsistency for CCFTs; the limit for CCFTs is inversely proportional to the square root of the yield strength while that for noncomposite circular HSS is inversely proportional to the yield strength. Moreover, comparison of the actual values for the most common materials reveals that the limit for composite sections is lower than that for noncompact (or compact) noncomposite sections. The general form of the equation for the elastic critical stress for local buckling of a circular section is given by (Roark and Young, 1975),

$$F_{cr} = \frac{E}{\sqrt{3}\sqrt{1-v^2}} \frac{2t}{D} \quad (11)$$

This indicates that the form of the equation given previously (AISC, 1993) was incorrect. To address this issue, the 1999 AISC *Specification* (AISC, 1999) gave the following limit for demarcating noncompact and slender tubes for local buckling in CCFTs,

$$\frac{D}{t} \leq 0.11 \frac{E}{F_y} \quad (12)$$

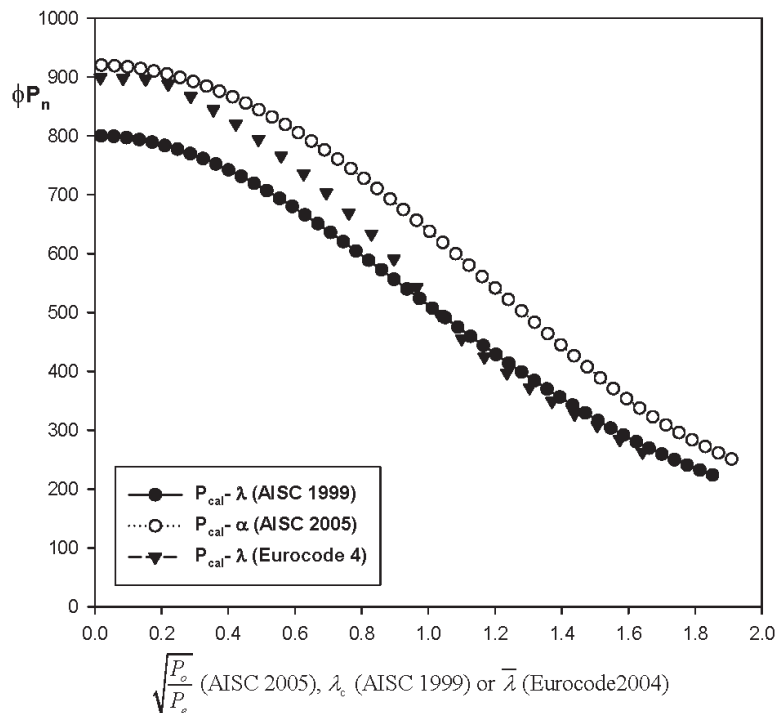


Fig. 10. Comparison of strength for a beam-column.

Table 3. Comparison of CFT Width-to-Thickness Ratio Limits for Local Buckling

Section	Type	AISC 1993		AISC 2005	
		Width-thickness limit	$F_y = 42$ ksi	Width-thickness limit	$F_y = 46$ ksi
Circular	Composite	$\frac{D}{t} < \sqrt{\frac{3E}{F_y}}$	$\frac{D}{t} < 74.3$	$\frac{D}{t} \leq 0.15 \frac{E}{F_y}$	$\frac{D}{t} < 103.6$
	Compact, noncomposite	$\frac{D}{t} < \frac{1,300}{F_y}$	$\frac{D}{t} < 30.9$	$\frac{D}{t} \leq 0.045 \frac{E}{F_y}^*$	$\frac{D}{t} < 31.1$
	Noncompact, noncomposite	$\frac{D}{t} < \frac{3,300}{F_y}$	$\frac{D}{t} < 78.6$	$\frac{D}{t} \leq 0.11 \frac{E}{F_y}$	$\frac{D}{t} < 76.0$
Rectangular	Composite	$\frac{b}{t} < \sqrt{\frac{3E}{F_y}}$	$\frac{b}{t} < 43.5$	$\frac{b}{t} < 2.26 \sqrt{\frac{E}{F_y}}$	$\frac{b}{t} < 56.7$
	Compact, noncomposite	$\frac{b}{t} < \frac{190}{\sqrt{F_y}}$	$\frac{b}{t} < 28.1$	$\frac{b}{t} < 1.12 \sqrt{\frac{E}{F_y}}$	$\frac{b}{t} < 28.1$
	Noncompact, noncomposite	$\frac{b}{t} < \frac{238}{\sqrt{F_y}}$	$\frac{b}{t} < 35.1$	$\frac{b}{t} < 1.40 \sqrt{\frac{E}{F_y}}$	$\frac{b}{t} < 35.1$

* This limit does not appear in the 2005 *Specification*. It was taken from the 1993 *LRFD Specification for Structural Steel Buildings* (AISC, 1993).

This was the same value used for noncomposite noncompact sections. This equation also reflects a major editorial change in the format of the equations, which was to nondimensionalize the limits by including the modulus of elasticity in the equations. Thus Equation 12 can be derived by multiplying the limit given in AISC (1993) by unity in the form of $E/29,000$ ksi:

$$\frac{D}{t} < \left(\frac{3,300}{F_y} \right) \left(\frac{E}{29,000} \right) = 0.11 \frac{E}{F_y} \quad (13)$$

The relaxation of the limits for CFT members in AISC (2005b) shown in Table 3 arises from two factors. The first factor is the recognition that the concrete infill reduces the problem of local buckling by forcing the buckled shape from that shown in Figure 11(a) (unfilled tube case) to that in Figure 11(b) (filled tube case). Figure 11 is only a schematic for the buckling of the steel skin in a circular shape subjected to uniform axial load, as the buckling length can differ considerably for the two cases shown. The different boundary

conditions at the end of the buckle and the associated buckling lengths lead to differences in the load required to create local buckling. The second factor is that considerably more data than was available for SSRC TG20 (SSRC, 1979) is now available for calibration, thus allowing for a more rational assessment of the slenderness limits that can be used in design.

When considering a circular section with continuous support on one side, the buckling mode is similar to that in Figure 11(b) and Figure 12 in plan. Bradford, Loh and Uy (2002) have shown that the theoretical solution to this case is very similar to Equation 11, except that the $\sqrt{3}$ term disappears from the denominator. Thus, from the theoretical standpoint, the slenderness limit is increased by a factor of 1.73 from the hollow case. However, it appears reasonable and conservative to assume that the $\sqrt{3}$ multiplier will apply to the design limit, bringing the multiplier in Equation 12 from 0.11 to almost 0.18. Because of the dearth of data on very slender CFTs, the increase in the local buckling limit was limited to 0.15 for circular CFTs relative to the local

buckling limit demarcating noncompact and slender circular hollow structural sections. In particular, based on a limited calibration, Bradford et al. (2002) recommended that the local buckling limit for CCFTs be set at,

$$\lambda = 125 \geq \left(\frac{D}{t}\right) \left(\frac{F_y}{250}\right) \quad (F_y \text{ in MPa})$$

Nondimensionalizing this recommendation, one obtains,

$$125 \left(\frac{250}{F_y}\right) \left(\frac{E}{200,000}\right) = 0.156 \left(\frac{E}{F_y}\right) \geq \left(\frac{D}{t}\right)$$

The constant at the front of the equation was then rounded to 0.15 in the 2005 AISC *Specification* (AISC, 2005b).

A major difference in the behavior of CCFT as compared to RCFT is that because the problem is axisymmetric for a CCFT, there is no possibility of redistribution of forces once buckling starts. Thus the post-buckling strength for this case is zero if one follows the classical von Karman formulation. It should be noted with reference to Figure 13 that the buckling for a RCFT involves only a part of the total width of the plate. Thus a redistribution of forces can occur after buckling begins. This redistribution is the primary source of the substantial post-buckling strength typical of rectangular plates. For a flat plate supported along one side, which can

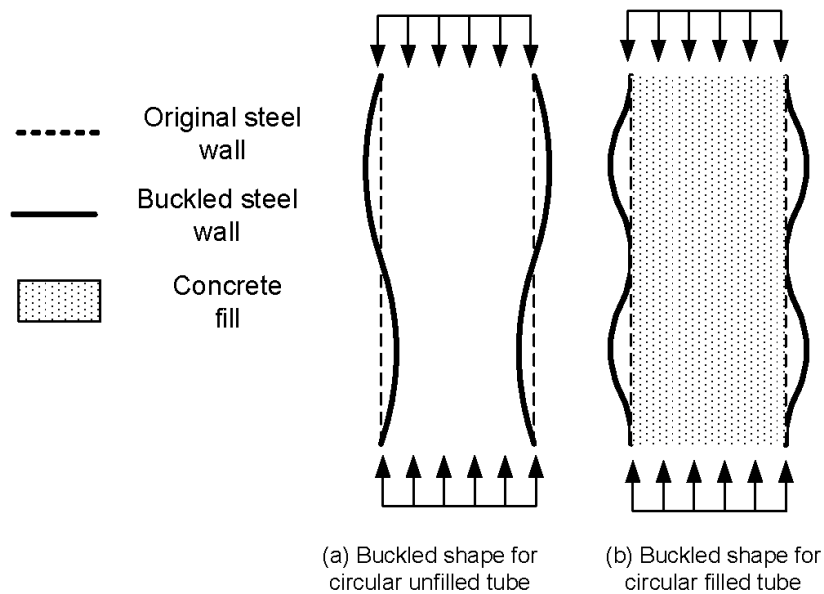


Fig. 11. Buckling shapes: (a) unrestrained from both sides and (b) restrained from one side.

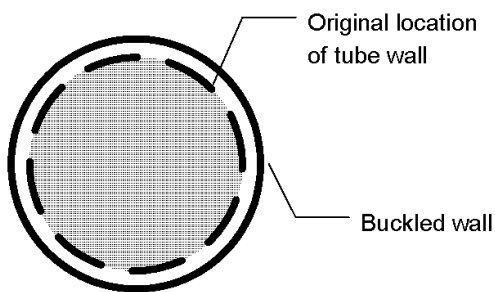


Fig. 12. Local buckling in a cylindrical tube (plan view).

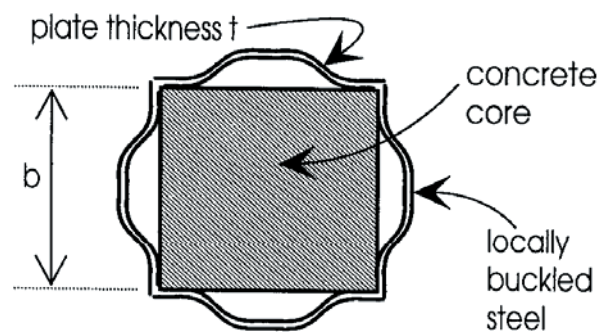


Fig. 13. Local buckling in a filled rectangular tube (Oehlers and Bradford, 1995).

be used to model one side of a rectangular HSS, the elastic critical buckling stress is given by the well known equation (Roark and Young, 1975),

$$F_{cr} = k \frac{\pi^2 E}{12 \sqrt{(1-\nu^2)} \left(\frac{b}{t}\right)^2} \quad (14)$$

where

- k = constant that accounts for the boundary conditions
- b = characteristic width

Equation 14 corresponds to the buckling shape shown in Figure 11(a) when k is taken as 4 (in other words, the plate is simply supported along its sides and no out-of-plane restraints exist). When a continuous support out-of-plane is added on one side, Uy and Bradford (1996), among others, have shown that for a rectangular plate, k becomes 10.67 or about 2.67 times that of the unfilled case [Figure 11(b) and Figure 13]. The values given by Equation 14 are not usable for design, as the effects of initial imperfections, residual stresses and other issues need to be addressed. Calibration to existing data for the case shown in Figure 11(a) has led to the limit of $1.40\sqrt{E/F_y}$ given in AISC (2005b) for noncomposite sections (SSRC, 1998). Thus, theoretically the 1.40 constant could be increased by up to 2.67 times, to 3.74. Based on available experimental data and other theoretical studies, the constant was increased to 2.26.

SHEAR STRENGTH

Another innovation in the 2005 *Specification* is the inclusion of explicit provisions for the calculation of the shear strength of composite columns. This issue is not as simple as it may appear at first as the contributions of the steel and concrete cannot be summed unless both reach their ultimate shear strength simultaneously. This would require that the shear strains in each material fall within a narrow range as the member reaches its ultimate strength, a difficult constraint to ensure given the incompatibilities of strains likely to occur as the member reaches failure. Thus AISC (2005b) offers two approaches. In the first, the column is treated as a regular reinforced concrete column, with the steel contribution coming only from any ties or stirrups present. The contribution of the webs of any steel section is ignored in this calculation. In the second method, the concrete contributions are ignored and only those of the webs of steel sections are considered. There is little data available on shear-critical composite columns tested under monotonic loads. There is a considerable amount of data in this area, mostly from Japan, for the case of cyclic loads. For all these reasons, future improvements to these provisions in future editions of the AISC *Specification* (AISC, 2005b) are warranted.

BOND TRANSFER

With respect to bond transfer, the provisions for SRC members were retained from the previous LRFD specification (AISC, 1999). With respect to CFTs, for the large majority of cases, bond strength is an issue in composite beam-columns only in localized regions near the connection of steel girders to CFTs, and then only if the steel girder is attached only to the steel tube without directly engaging the concrete core. Away from the connection, any amount of flexure engages the concrete sufficiently to help ensure load transfer along the length, generally filling any gaps due to shrinkage. The AISC (2005) provisions and commentary are written with this as a consideration. For CFTs the provisions clarify that stress transfer between the constituent materials should be calculated based on direct bond interaction, shear connection, or direct bearing; the mechanism that yields the largest nominal strength may be used, but the experimental evidence (for example, Shakir-Khalil, 1993) clarifies that summation of the strengths of these mechanisms is not justified. With this in mind, the bond strength from experiments of RCFTs is found to be approximately (Hajjar, 2000):

- 0.015 to 0.058 ksi (0.1 to 0.4 MPa) for tests in which the steel tube is pushed past the concrete core, with reasonably low scatter and a mean value of 0.036 ksi (0.25 MPa).
- 0.015 to 0.15 ksi (0.1 to 1.0 MPa) for tests in which the concrete core is pushed past the steel tube, with reasonably high scatter (a mean value is unavailable at this time).
- 0.058 to 0.15 ksi (0.4 to 1.0 MPa) for tests in which shear tabs are attached to the middle of the rectangular CFT and shear is applied to the shear tabs, thus introducing eccentricity of the load at the point of load introduction, with a mean value of approximately 0.087 ksi (0.6 MPa).
- Summary: Assuming a bond strength of 0.022 ksi (0.15 MPa) is probably conservative. Assuming a bond strength of 0.058 ksi (0.4 MPa) is above many of the push-out tests, but is reasonable if one assumes that there is at least some eccentricity occurring at all points of load introduction. Eurocode 4 assumes a bond strength of 0.058 ksi (0.4 MPa). The Japanese code assumes a bond strength of 0.022 ksi (0.15 MPa).

The bond strength from experiments on CCFTs is approximately:

- 0.015 to 0.058 ksi (0.1 to 0.4 MPa) for tests in which the steel tube is pushed past the concrete core, with reasonably low scatter and a mean value of 0.044 ksi (0.30 MPa). Figure 14 (1 ksi = 6.895 MPa) shows data for pushout experiments, where the concrete core is pushed through the steel skin in order to assess bond characteristics.

- 0.015 to 0.15 ksi (0.1 to 1.0 MPa) or higher for tests in which the concrete core is pushed past the steel tube, with reasonably high scatter (a mean value is unavailable at this time).
- 0.058 to 0.15 ksi (0.4 to 1.0 MPa) for tests in which shear tabs are attached to the middle of the CCFT and shear is applied to the shear tabs, thus introducing eccentricity of the load at the point of load introduction, with a mean value of approximately 0.087 ksi (0.6 MPa).
- Summary: Assuming a bond strength of 0.022 ksi (0.15 MPa) is probably conservative. Assuming a bond strength of 0.058 ksi (0.4 MPa) is above some of the push-out tests, but is reasonable if one assumes that there is at least some eccentricity occurring at all points of load introduction. Eurocode 4 assumes a bond strength of 0.058 ksi (0.4 MPa).

It is not clear what percentage of the CFT perimeter is typically engaged for transferring the load. The width of the tube flange is reasonable for an RCFT, and is assumed here. Assuming half the perimeter of an RCFT may also be reasonable, although out-of-plane connections may influence that behavior. Similarly, assuming one-quarter of the perimeter of a CCFT is probably reasonable, but conservative. Assuming half the perimeter of a CCFT may also be reasonable, and is assumed here, although out-of-plane connections may influence that behavior. It is also not clear what distance along the CFT length is typically engaged for transferring the load, before the load is shared between the concrete and steel in proportion to their rigidities. Reported ranges have

varied from $0.5b$ to $2.75b$ above and below the connection for rectangular CFTs, and from $0.25D$ to $1.0D$ above and below the connection for CCFTs, where b is the flange width (rectangular) and D is the diameter (circular), respectively.

Summary

The above information indicates that the CFT provisions that are potentially justifiable may have results that vary by *an order of magnitude*. For example, the following are reasonable scenarios for a rectangular CFT (circular would be similar):

- Nominal bond strength of 0.022 ksi (0.15 MPa), with a nominal bond area of $b(0.5b)$ above and below the connection, where b is the flange width of a rectangular CFT. This is very conservative.
- Nominal bond strength of 0.058 ksi (0.4 MPa), with a nominal bond area of $b(0.5b)$ above and below the connection, where b is the flange width of a rectangular CFT.
- Nominal bond strength of 0.058 ksi (0.4 MPa), with a nominal bond area of $b(1.0b)$ above and below the connection, where b is the flange width of a rectangular CFT.
- Nominal bond strength of 0.058 ksi (0.4 MPa), with a nominal bond area of $(b + d)(0.5b)$ above and below the connection, where b is the flange width and d is the flange depth of a rectangular CFT.

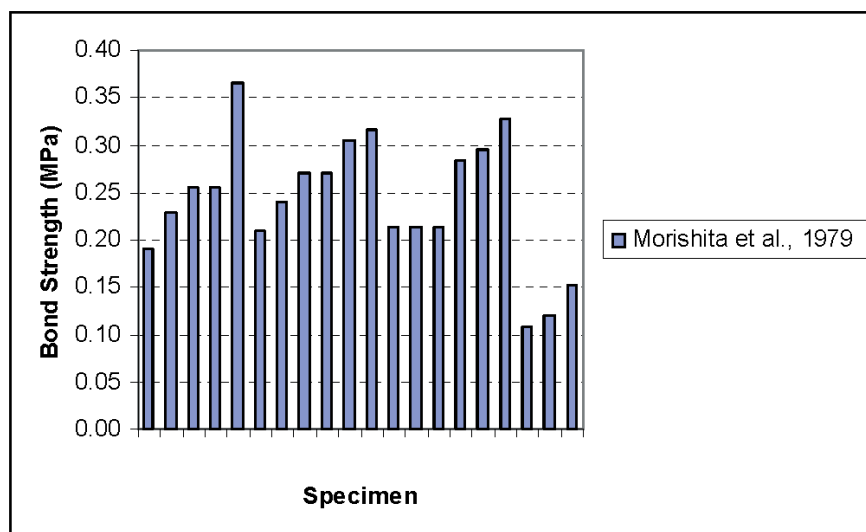


Fig. 14. Histogram for bond strength from push-out experiments for rectangular specimens tested by Morishita et al. (1979).

Table 4. Comparison of Material and Detailing Provisions in ANSI/AISC 360-05 (AISC, 2005b) vs. ACI (ACI, 2005) for CFTs

Item	AISC 2005	ACI 2005 Conflicts/Issues
Material Limitations	<ul style="list-style-type: none"> • $3 \text{ ksi} \leq f'_c \leq 10 \text{ ksi}$ (NW) • $3 \text{ ksi} \leq f'_c \leq 6 \text{ ksi}$ (LW) • $F_y \leq 75 \text{ ksi}$ • Larger f'_c permitted for stiffness calculations 	<ul style="list-style-type: none"> • $f'_c > 2.5 \text{ ksi}$ (both NW and LW) • $F_y < 80 \text{ ksi}$ for spiral reinforcement • $F_y < 50 \text{ ksi}$ for steel shapes • Upper limit of 10 ksi on shear and bond provisions, and f_t definitions are provided for lightweight concrete
Minimum transverse reinforcement	$\geq 0.009 \text{ in.}^2$ per in. of tie spacing.	$\rho_s = 0.54 \left(\frac{A_g}{A_{ch}} - 1 \right) \frac{f'_c}{f_{yt}}$ for spirals; controlled by spacing/minimum diameter for rectangular ties and by $A_{v,\min} = 0.75 \sqrt{f'_c} \frac{b_w s}{f_{yt}}$
Local Buckling	$b/t < 2.26 \sqrt{E/F_y}$ (rectangular) $D/t < 0.15E/F_y$ (circular)	$b/t < \sqrt{\frac{3E}{F_y}} = 1.73 \sqrt{\frac{E}{F_y}}$ (rectangular) $D/t < \sqrt{\frac{8E}{F_y}}$ (circular)
Reinforcement Ratio	1% for the steel core plus 0.4% for continuous longitudinal bars	$1\% < \rho_s < 8\%$ plus steel shape (with no upper limit)

NW = normal weight concrete ; LW = lightweight concrete

- Nominal bond strength of 0.058 ksi (0.4 MPa), with a nominal bond area of $(b+d)(1.0b)$ above and below the connection, where b is the flange width and d is the flange depth of a rectangular CFT. This estimate is approximately 10 times larger than the first estimate above. This estimate is potentially unconservative, although still reasonable.

As a compromise, it is recommended to use

$$(0.058 \text{ ksi})(b)(1.0b) [(0.4 \text{ MPa})(b)(1.0b)]$$

However, this would cause many girder-to-CFT connections to require shear connectors or direct bearing, even for small CFTs.

Note that while circular CFTs may have shorter transfer lengths, they are likely to have higher bond strengths. This fact justifies the provisions being written similarly for rectangular and circular CFTs. Thus, the provisions for rectangular CFTs assume that one face resists the shear, while the provisions for circular CFTs assume that one-half the perimeter resists the shear, but both use the same bond strength and same distance along the length for the shear resistance.

The value of ϕ is calibrated to the circular push-out tests of Morishita, Tomii and Yoshimura (1979) assuming a reli-

ability index of 3.0; the tests of Morishita et al. (1979) had a mean bond strength of approximately 0.3 MPa and a coefficient of variation of approximately 0.30. The values for rectangular CFTs were a little lower, yielding an unreasonably low value of ϕ of approximately 0.38. As there is enough scatter in the data, using the same value of $\phi = 0.45$ for both rectangular and circular CFTs seems warranted. If the ratio of mean to nominal bond strength is taken as 1.0, the value of ϕ is 0.60.

Little guidance is currently given for where to place the shear connectors, or what the maximum shear connector spacing may be, or whether there is a minimum limit on tube thickness for attaching shear connectors. As a minimum aid, it is recommended that the shear connectors be distributed over an area that is 2.5 times longer than the area assumed for the calculation of the nominal bond strength.

For SRC members, a new provision was also added for the strength of the stud connectors. While experimental evidence is beginning to build to justify development of specific equations for shear connector strength in SRC members, for simplicity an equation for computing shear connector strength is retained for SRC members that is similar to that used for composite beams (but without including factors that are dependent on metal deck).

COMPARISON OF AISC AND ACI COMPOSITE COLUMN DESIGN PROVISIONS

Because one of the objectives of this work was to examine and, where possible, reduce differences between current ACI and AISC provisions, this section presents a short discussion of issues that an ad-hoc joint AISC-ACI committee on composite construction will be addressing in the future. As noted earlier, differences in calculation of the basic cross-section strength have been significantly reduced. The method proposed in ANSI/AISC 360-05 (AISC, 2005b) is in compliance with the requirements in ACI 318 (ACI, 2005) Sections 10.2 and 10.3, so it can be argued that in effect this difference has been bridged. However, there is still a need to resolve the issue of when and how to include time effects (creep and shrinkage) in design calculations. Currently ACI applies a factor $(1 + \beta_d)$ in the denominator in calculating the moment of inertia for both the determination of forces and displacements and stability calculations. AISC does not directly address this issue; although designers are warned that time effects need to be considered. There is a need to revisit the definition of time effects for members with relatively large reinforcement ratios. The current ACI definition for β_d does not take into account reinforcement ratio, but creep should typically be less of a problem in a column with a large reinforcement ratio if a continuous steel shape is present. In addition, ACI does not give any credit for confinement in concrete-filled circular sections, while AISC does by allowing use of $0.95f'_c$ as opposed to $0.85f'_c$ in Equation (AISC-I2-13). The issue of confinement in circular concrete-filled steel tubes is one in which both codes need to make further advances. There are also still significant but not irreconcilable differences in the material and detailing requirements by both specifications, as summarized in Table 4. Table 4 summarizes the current ANSI/AISC 360-05 (AISC, 2005b) requirements in the second column and highlights differences in ACI 318 (ACI, 2005) relative to AISC 2005 in the third column.

CONCLUSIONS

This paper has summarized the background information for composite columns and beam-columns, including both steel reinforced concrete (SRC) and concrete-filled steel tube (CFT) members, relevant to new provisions in the 2005 AISC *Specification* (AISC, 2005b). New provisions are included for:

- Composite column axial compressive strength
- Local buckling strength of concrete-filled steel tubes
- Shear strength of composite members
- Bond transfer between the steel and concrete materials for concrete-filled steel tubes

The 2005 AISC *Specification* (AISC, 2005) also includes new provisions for composite members in axial tension, in which the strength of the steel section alone is utilized. Together, these provisions greatly augment the breadth of applicability of design provisions for composite columns and beam-columns and provide information based upon the latest data in the literature.

ACKNOWLEDGMENTS

This research was sponsored by the National Science Foundation under Grant No. CMS-0084848, the American Institute of Steel Construction, the Georgia Institute of Technology, the University of Minnesota, and the University of Illinois at Urbana-Champaign. The authors would like to thank the members of AISC Specification Task Committee 5 on Composite Construction for their contributions to this research. The assistance of Lawrence A. Griffis and Cenk Tort are gratefully acknowledged.

REFERENCES

- Aho (1997), "A Database for Encased and Concrete-Filled Columns," M.S. Thesis, Graduate School, The Georgia Institute of Technology, Atlanta, GA.
- ACI (2005), *Building Code Requirements for Structural Concrete*, ACI 318-05, American Concrete Institute, Farmington Hills, MI.
- AISC (1993), *Load and Resistance Factor Design Specification for Structural Steel Buildings*, December 1, 1993, American Institute of Steel Construction, Inc., Chicago, IL.
- AISC (1999), *Load and Resistance Factor Design Specification for Structural Steel Buildings*, December 27, 1999, American Institute of Steel Construction, Inc., Chicago, IL.
- AISC (2005a), *Seismic Provisions for Structural Steel Buildings*, ANSI/AISC 341-05, March 9, 2005, American Institute of Steel Construction, Inc., Chicago, IL.
- AISC (2005b), *Specification for Structural Steel Buildings*, ANSI/AISC 360-05, March 9, 2005, American Institute of Steel Construction, Inc., Chicago, IL.
- AISC (2005c), *Steel Construction Manual*, 13th Edition, American Institute of Steel Construction, Inc., Chicago, IL.
- Bradford, M.A., Loh, H.Y., and Uy, B. (2002), "Slenderness Limits for Filled Circular Steel Tubes," *Journal of Constructional Steel Research*, Vol. 58, pp. 243–252.
- Chien, E. Y. L. and Ritchie, J. K. (1984), *Design and Construction of Composite Floor Systems*, Canadian Institute of Steel Construction, Toronto, Canada, August.

- Chien, E. Y. L. and Ritchie, J. K. (1993). "Composite Floor Systems—A Mature Design Option," *Journal of Constructional Steel Research*, Vol. 25, Nos. 1–2, pp. 107–139.
- Deierlein, G.G., and Leon, R.T. (1998), "Future Trends in Composite Construction," *Hybrid and Composite Construction*, ACI SP 174, ACI International, Farmington Hills, MI, pp. 113–138.
- Eurocode (2004), EN 1994: Design of Composite Steel and Concrete Structures: Part 1.1: General Rules and Rules for Buildings, Eurocode 4, EN 1994-1-1:2004, CEN, Brussels (supersedes ENV 1994-1-1:1992).
- Galambos, T.V. (2000), "Recent Research and Design Developments in Steel and Composite Steel-Concrete Structures in USA," *Journal of Constructional Steel Research*, Vol. 55, No. 1–3, July–September, pp. 289–303.
- Hajjar, J.F. (2000), "Concrete-Filled Steel Tube Columns under Earthquake Loads," *Progress in Structural Engineering and Materials*, Vol. 2, No. 1, pp. 72–82.
- Hansell, W.C., Galambos, T.V., Ravindra, M.K., and Viest, I.M. (1978), "Composite Beam Criteria in LRFD," *Journal of the Structural Division*, ASCE, Vol. 104, No. ST9, September, pp. 1409–1426.
- Kim, D.K. (2005), "A Database for Composite Columns," M.S. Thesis, Graduate School, The Georgia Institute of Technology, Atlanta, GA.
- Leon, R.T. and Bawa, S. (1990), "Performance of Large Composite Columns," *Proceedings of the IABSE Symposium on Mixed Structures*, Zurich, pp. 179–184.
- Leon, R.T. and Bawa, S. (2002), "Measurements on a Large Composite Column During Construction," in *Theorie und Praxis im Konstruktiven Ingenieurbau*, Festschrift Prof. Dr.-Ing. H. Bode, Ibidem, Stuttgart, pp. 237–250.
- Leon, R.T. and Aho, M.F. (2002), "Toward New Design Provisions for Composite Columns," *Composite Construction in Steel and Concrete IV*, Hajjar, J.F., Hosain, M., Easterling, W.S., and Shahrooz, B.M. (eds.), American Society of Civil Engineers, Reston, VA, pp. 518–527.
- Leon, R.T. and Hajjar, J.F. (2007), "Background to Composite Column Design Changes in the 2005 AISC Specification," SEMM Report 07-12, School of Civil and Environmental Engineering, Georgia Tech, Atlanta, GA.
- Lundberg, J.E. (1993), "The Reliability of Composite Columns and Beam-Columns," Structural Engineering Report No. 93-2, Department of Civil and Mineral Engineering, University of Minnesota, Minneapolis, MN.
- Lundberg, J.E. and Galambos, T.V. (1996), "Load and Resistance Factor Design of Composite Columns," *Structural Safety*, Vol. 18, No. 2–3, pp. 169–177.
- Morino, S., Uchikoshi, M. and Yamaguchi, I. (2001), "Concrete-Filled Steel Tube Column System—Its Advantages," *Steel Structures*, Vol. 1, pp. 33–44.
- Morishita, Y., Tomii, M. and Yoshimura, K. (1979), "Experimental Studies on Bond Strength in Concrete-Filled Square and Octagonal Steel Tubular Columns Subjected to Axial Loads," *Transactions of the Japan Concrete Institute*, Vol. 1, pp. 359–366.
- Mirza S.A. and Tikka, T. (1999), "Flexural Stiffness of Composite Columns Subjected to Major Axis Bending," *ACI Structural Journal*, Vol. 96, No. 1, January–February, pp. 19–28.
- Oehlers, D. and Bradford, M.A. (1995), *Composite Steel and Concrete Structural Members*, Pergamon Press, Oxford, United Kingdom, 549 pp.
- Ravindra, M.K. and Galambos, T.V. (1978), "Load and Resistance Factor Design for Steel," *Journal of the Structural Division*, ASCE, Vol. 104, No. ST9, September, pp. 1337–1354.
- Roark, R.J. and Young, W.C. (1975), *Formulas for Stress and Strain*, 5th Ed., McGraw-Hill, New York, 624 pp.
- Roeder, C.W. (1998), "Overview of Composite Systems for Seismic Design in the United States," *Engineering Structures*, Vol. 20, Nos. 4–6, pp. 355–363.
- Roik, K. and Bergmann, R. (1988), Eurocode 4: Composite Columns, Report EC4/6/89, U. of Bochum, Bochum.
- Roik, K. and Bergmann, R. (1992), "Composite Columns," *Constructional Steel Design*, Dowling, P., Harding, J. E., and Bjorhovde, R. (eds.), Elsevier Science Publishers, New York, pp. 443–470.
- Shakir-Khalil, H. (1993), "Resistance of Concrete-Filled Steel Tubes to Pushout Forces," *The Structural Engineer*, Vol. 71, No. 13, pp. 234–243.
- SSRC (1979), "A Specification for the Design of Steel-Concrete Composite Columns," Structural Stability Research Council Task Group 20 (SSRC TG20), *Engineering Journal*, AISC, Vol. 16, No. 4, Fourth Quarter, pp. 101–115.
- SSRC (1998), *Guide to Stability Design Criteria for Metal Structures*, Galambos, T. V. (ed.), 5th Ed., Structural Stability Research Council, John Wiley and Sons, New York.
- Smith, B.S. and Coull, A. (1991), *Tall Building Structures: Analysis and Design*, John Wiley & Sons, New York, NY.
- Taranath, B.S. (1998), *Steel, Concrete, and Composite Design of Tall Buildings*, McGraw-Hill, New York, NY.
- Uy, B. and Bradford, M.A. (1996), "Elastic Local Buckling of Steel Plates in Composite Steel-Concrete Structures," *Engineering Structures*, Vol. 18, No.3, pp. 193–200.
- Uy, B. (1998), "Ductility, Strength and Stability of Concrete-Filled Steel Box Columns for Tall Buildings," *Structural Design of Tall Buildings*, Vol. 7, No. 2, June, pp. 113–133.
- Viest, I.M., Colaco, J.P., Furlong, R.W., Griffis, L.G., Leon, R.T. and Wyllie, Jr., L.A. (1997), *Composite Construction: Design for Buildings*, McGraw-Hill, New York, NY.